7 Zelen, M., "Multi-Factor Experiments for Evaluating Reliability," Nov. 1957 (to be published in the open literature).
8 Epstein, B., and Sobel, M., "Life Testing," *Journal of the American Statistical Association*, 1953, pp. 486–502.
9 Sobel, M., "Statistical Techniques for Reducing the Experiment Time in Reliability Studies," *Bell System Technical Journal*, vol. XXXV, no. 1, 1956, pp. 179–202.
10 Parsons, J. H., Wong, K. L., and Yeiser, A. S., "Statistics of Electronic System Failures," IRE Convention Record, Part 6, 1955, pp. 69–73.
11 Gunn, W. A., "The Reliability of Complex Systems," Western Regional Conference Proceedings ASQC, Aug. 20–21, 1956.
12 Lipow, M., "A Unified Model for Catastrophic Failure," Western Regional Conference Proceedings ASQC, Sept. 9–10, 1957.
13 Molina, E. C., "Poisson's Exponential Binomial Limit," Van Nostrand, New York, 1942.
14 Weiss, G. H., "On the Theory of Replacement of Machinery with Random Failure Time," Ballistic Research Laboratories, Aberdeen Proving Ground, Report 982, March 1956.
15 Meltzer, S. A., "Statistical Analysis of Equipment Reliability," Radio Corporation of America EM 4194, June 1955.
16 Acheson, M. A., "The Whole Is Not the Sum of Its Parts," Fourth National Symposium on Reliability and Quality Control in Electronics, Jan. 6–8, 1958.
17 Geckler, R. D., "The Principles of Developing Solid-Propellant Rockets," Aerojet-General TM 220, June 1953 (unclassified excerpts from reference; main document classified).
18 Del Priore, F. R., and Day, B. B., "The Engineer and Statistician Can Meet," NAVORD Report 4028, 1953.
19 Box, G. E. P., "Evolutionary Operation," Proceedings of the Symposium on Design of Industrial Experiments, Institute of Statistics, University of North Carolina, Nov. 5–9, 1956.

Additional References

20 Breakwell, J. V., "Economically Optimum Acceptance Tests," *Journal of the American Statistical Association*, vol. 51, June 1956, p. 243.
21 Howard, W. J., "A Simple Failure Model for Complex Mechanisms," The Rand Corp., Report RM-1058 March 1953.
22 Lawrence, H. R., and Amster, W. H., "Reliability Achievement and Demonstration in a Development Program," Space Technology Laboratories, Ramo-Wooldridge Corp. (to be published).

Exhaust Nozzle Contour for Optimum Thrust

G. V. R. RAO[1]

Marquardt Aircraft Co., Van Nuys, Calif.

A method for designing the wall contour of an exhaust nozzle to yield optimum thrust is established. The nozzle length, ambient pressure and flow conditions in the immediate vicinity of the throat appear as governing conditions under which the thrust on the nozzle is maximized. Isentropic flow is assumed and the variational integral of this maximizing problem is formulated by considering a suitably chosen control surface. The solution of the variational problem yields certain flow properties on the control surface, and the nozzle contour is constructed by the method of characteristics to give this flow. An example is carried out and typical nozzle contours are given.

Nomenclature

A	=	cross-sectional area of nozzle
F_i, f_i, G_i	=	various functions defined in the text, with $i = 1, 2, 3$
h	=	Lagrangian multiplier, which is a function of y
L	=	length of the nozzle
M	=	Mach number
p	=	local pressure
p_a	=	ambient pressure
W	=	flow velocity (scalar)
x	=	coordinate in the axial direction
y	=	coordinate in the radial direction
α	=	Mach angle
γ	=	ratio of specific heats
δ	=	variation
θ	=	angle between flow direction and nozzle axis
λ_2, λ_3	=	Lagrangian multiplier constants
ρ	=	density
ϕ	=	angle between control surface and nozzle axis

Subscripts

c	=	chamber conditions
C, E, F	=	values taken at respective points
M, θ	=	denote partial differentiation
t	=	conditions at throat

Presented at the ARS Semi-Annual Meeting, San Francisco, Calif., June 10–13, 1957.

[1] Research Scientist. Now with Rocketdyne, Canoga Park, Calif.

Introduction

THE diverging portion of an exhaust nozzle is an important feature for all engines which depend upon the thrust produced by the exhaust gases. Maximum possible thrust on a nozzle can be obtained by complete expansion of the exhaust gases to the ambient pressure through a nozzle designed to give a parallel uniform jet at the exit. One may apply the method suggested by Foelsch (1)[2] for the design of such nozzles. For jet engines operating at high altitudes and especially for rocket motors, one is required to design nozzles for very low ambient pressures. Even the shortest nozzle designed by the aforementioned method would be excessively long and heavy. Logically, one would seek a nozzle of limited length, since length is a fair indication of nozzle weight. The problem then is the choice of a nozzle having a specified length and yielding maximum thrust. Semi-empirical investigations of this problem were carried out by Dillaway (2) and Fraser and Rowe (3). A mathematically rigorous formulation and some numerical examples are due to Guderley and Hantsch (4). Their principal idea is the introduction of a characteristic surface as control surface for the momentum, the mass flow and the length of the nozzle. By this choice, the partial differential equations governing the gas flow reduce to one ordinary differential equation, and a one-dimensional variational problem is obtained.

The present paper proceeds in a similar fashion but does not specify in advance that the control surface is a characteristic surface. The form of the control surface and the velocity distribution along it are determined in such a manner that the thrust assumes a maximum, while the mass flow has a constant value. Obviously, this formulation fails to include an expression for the flow differential equations, and thus one might be in doubt if the velocity distribution along the control surface thus obtained can occur within an actual flow. However, one finds that the control surface becomes automatically a characteristic surface. For this reason, the characteristic conditions need not be included in the present formulation.

[2] Numbers in parentheses indicate References at end of paper.

This results in a great reduction of the computational work. Moreover, the approach shown here may possess a mathematical interest of its own.

Initial Expansion in the Nozzle

Let $ATBE$, as shown in Fig. 1(a), represent the intersection of the nozzle contour with the meridional plane. Contour AT is the contraction upstream of the throat and TBE is the diverging portion of the nozzle. The initial expansion occurs along TB and the wall contour B to E turns the flow back to a direction nearer the axial. Guderley and Hantsch considered this initial expansion to occur through a sharp corner. Since it is advisable to avoid sharp corners in exhaust nozzle contours, one can prescribe a suitable contour TBB' in the throat region. However, the location of point B along this prescribed curve is left open in considering various nozzle shapes. The location of point B, in fact, is a part of the solution of the problem. After the point B is determined the contour BB' does not effect the construction of the optimum nozzle contour.

Sauer (5) gives a method of analyzing transonic flow in the throat region in terms of the radius of curvature of the nozzle wall at the throat. Using this method, a line TT' (Fig. 1(a)) can be defined along which the Mach number is constant. The flow directions at various locations along the line can be computed. In the few examples carried out by the author, the Mach number along TT' was larger than unity and no difficulty was encountered in applying the method of characteristics to determine the flow downstream of the line TT'.

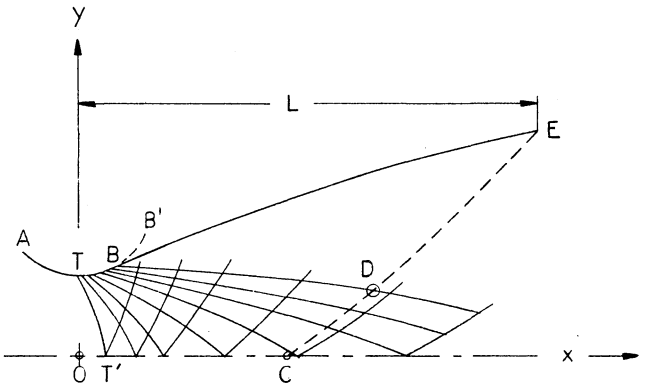

Fig. 1(a) Characteristics net and control surface

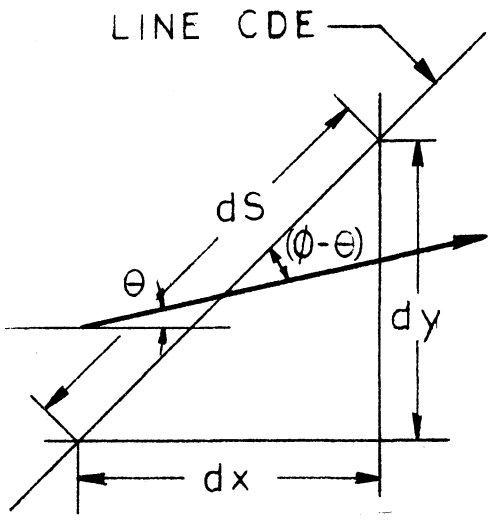

Fig. 1(b) Flow across an element of control surface

The origin of the coordinate system lies at the throat section, the x-axis coincides with the nozzle axis, and y represents the radial distance from the nozzle axis. To construct the flow field a number of points between T and B' are chosen and the values of x, y and θ for the given contour are determined at these points. Using these initial conditions along TT' and TBB', the method of characteristics (6) can be applied to construct a characteristics net and evaluate flow properties at the net points. Such a net of characteristics is schematically shown in Fig. 1(a) and is denoted as the "kernel" since the variations in the nozzle shape between B and E do not alter the flow properties in the region upstream of right characteristic through B. Location of point B on the prescribed contour is implied in the determination of the last right characteristic up to which the "kernel" of Fig. 1(a) is to be utilized in the construction of the nozzle shape.

Formulation of the Problem

For computing thrust on the nozzle and mass flow through the nozzle, let us consider a control surface passing through the exit of the nozzle. In Fig. 1(a), let CE describe the intersection of the control surface with the meridional plane. Let ϕ, a function of y, denote the inclination of line CE to the nozzle axis. The location of the point C on the axis and the function $\phi(y)$ would then completely define the control surface. Along CE consider an elemental length ds (Fig. 1(b)) at a distance y from the nozzle axis. The elemental area generated by rotation about the axis is $dA = 2\pi y ds$. Also, $ds = dy/\sin\phi$.

Let ρ, W and θ denote respectively the density, velocity and flow direction considered uniform over the element ds. The mass flow crossing the elemental area is given by

$$\rho W \frac{\sin(\phi - \theta)}{\sin\phi} 2\pi y dy$$

and the momentum flux in the x direction

$$\rho W^2 \frac{\sin(\phi - \theta)\cos\theta}{\sin\phi} 2\pi y dy$$

By integrating along CE one obtains the mass flow crossing the control surface

$$\text{mass flow} = \int_C^E \rho W \frac{\sin(\phi - \theta)}{\sin\phi} 2\pi y dy \quad \ldots\ldots [1]$$

Similarly, thrust on the nozzle can be obtained by integrating pressure differential and momentum flux across CE

$$\text{thrust} = \int_C^E \left[(p - p_a) + \rho W^2 \frac{\sin(\phi - \theta)\cos\theta}{\sin\phi} \right] 2\pi y dy \quad \ldots. [2]$$

In the present problem the conditions at the inlet to the nozzle are assumed to be given and hence maximizing the above expression is sufficient.

The axial distance between C and E is given by

$$x_E - x_C = \int_C^E \cot\phi \, dy$$

Hence the length of the diverging portion of the nozzle is

$$\text{length} = x_C + \int_C^E \cot\phi \, dy \quad \ldots\ldots [3]$$

Varying the nozzle contour would involve corresponding variations in the control surface. One can leave point C fixed and vary ϕ to obtain the variations in the control surface. The location of the point C depends upon the length chosen for the nozzle. Point C can be treated as fixed in the present problem, since the variations of nozzle contour are subject

to constant length. Hence the following condition must be satisfied

$$\int_C^E \cot \phi \, dy = \text{const} \quad \ldots\ldots [4]$$

Continuity of mass flow requires that the mass flow as given by Equation [1] must be equal to mass flow through the throat section, which is invariant with changes in the nozzle contour. Hence it is required to maximize thrust on the nozzle subjected to the restrictions given by Equations [1, 4]. Using the Lagrangian multiplier method this problem can be reduced to maximizing the integral

$$I = \int_C^E (f_1 + \lambda_2 f_2 + \lambda_3 f_3) dy \quad \ldots\ldots [5]$$

where

$$f_1 = \left[(p - p_a) + \rho W^2 \frac{\sin (\phi - \theta) \cos \theta}{\sin \phi} \right] y$$

$$f_2 = \rho W \frac{\sin (\phi - \theta)}{\sin \phi} y$$

$$f_3 = \cot \phi$$

and λ_2, λ_3 are Lagrangian multiplier constants.

Solution of the Problem

The solution of the problem lies in setting the first variation of I (Equation [5]) equal to zero and thereby obtaining the required control surface and flow conditions along it. Let us first enumerate all the permissible variations of the quantities appearing in the integral. In the following discussion, δ denotes variation of a function, and partial derivatives are indicated by the respective subscripts.

As explained in the introduction, the initial expansion immediately behind the throat region is assumed to occur along a prescribed contour TBB' (Fig. 1(a)). Let B indicate the point up to which such an expansion takes place, and let the right characteristic from B intersect the control surface at D. Any variation in nozzle contour downstream of point B would not affect the flow between C and D.

For convenience the control surface between C and D is assumed to coincide with a left characteristic in the "kernel" of the characteristics net. This leads to δC, δM and $\delta\theta$ all zero in this region. $\phi = (\alpha + \theta)$ is a known quantity along CD, yielding $\delta\phi = 0$. The location of point D, i.e., the extent to which the assumed initial expansion occurs, is not known. Hence δD is not zero.

Between D and E, we have δD, δM, $\delta\theta$ and $\delta\phi$ all nonzero. Since only the length of the nozzle is prescribed, δy_E is nonzero. M and θ are continuous in the interior of the flow, and ϕ is also required to be continuous along CDE. Hence the integrand in Equation [5] is continuous. The variation of point D therefore does not enter into the first variation of the integral I, and one obtains

$$\delta I = 0 = \int_{y_D}^{y_E} \{(f_{1M} + \lambda_2 f_{2M} + \lambda_3 f_{3M})\delta M + (f_{1\theta} + \lambda_2 f_{2\theta} + \lambda_3 f_{3\theta})\delta\theta + (f_{1\phi} + \lambda_2 f_{2\phi} + \lambda_3 f_{3\phi})\delta\phi\} dy + \delta y_E (f_1 + \lambda_2 f_2 + \lambda_3 f_3)_{\text{at } E} \quad \ldots [6]$$

Since the variations in M, θ, ϕ and y_E are arbitrary, the above leads to

$$f_{1M} + \lambda_2 f_{2M} + \lambda_3 f_{3M} = 0 \quad \ldots\ldots [7]$$

$$f_{1\theta} + \lambda_2 f_{2\theta} + \lambda_3 f_{3\theta} = 0 \quad \ldots\ldots [8]$$

$$f_{1\phi} + \lambda_2 f_{2\phi} + \lambda_3 f_{3\phi} = 0 \quad \ldots\ldots [9]$$

along DE, and

$$f_1 + \lambda_2 f_2 + \lambda_3 f_3 = 0 \quad \text{at } E \quad \ldots\ldots [10]$$

Since f_{3M} and $f_{3\theta}$ are zero, one obtains from Equations [7, 8]

$$f_{1M} f_{2\theta} = f_{1\theta} f_{2M}$$

It should be noted that y drops out of the above equation, leading to

$$\phi = \theta + \alpha \quad \text{along } DE \quad \ldots\ldots [11]$$

This above relation shows that the control surface coincides with the last left characteristic in the nozzle flow, and the conditions along this line are obtained by introducing this relation into Equations [8, 9]. Hence

$$\frac{W \cos (\theta - \alpha)}{\cos \alpha} = -\lambda_2 \quad \ldots\ldots [12]$$

and

$$y\rho W^2 \sin^2 \theta \tan \alpha = -\lambda_3 \quad \ldots\ldots [13]$$

along DE are the necessary conditions for the integral [5] to be a maximum. Substituting Equations [11, 12, 13] into Equation [10], the following condition results

$$\sin 2\theta = \frac{p - p_a}{\frac{1}{2}\rho W^2} \cot \alpha \quad \text{at } E \quad \ldots\ldots [14]$$

This condition relating M and θ at the end point of the nozzle is the same as given in (4).

From Equations [12, 13] one can obtain the following relation dM/dy and $d\theta/dy$

$$\frac{d\theta}{dy} - \frac{\sqrt{M^2 - 1}}{M\left(1 + \frac{\gamma - 1}{2} M^2\right)} \frac{dM}{dy} + \frac{\sin \alpha \sin \theta}{y \sin (\theta + \alpha)} = 0 \quad \ldots [15]$$

This relation is the compatibility condition between the Mach number and the flow direction along a left characteristic. It is crucial to this approach that such a condition is implicit in the solution of Equations [12, 13], since according to Equation [11] the control surface has the direction of the left characteristic. If the condition of compatibility were not fulfilled, the control surface would become a limiting line, i.e., the flow pattern would be physically impossible. Equations [12, 13], in connection with [11], give the form of the control surface and the velocity distribution in a form which does not require the solution of partial differential equations. In this regard, the present paper goes beyond Guderley's solution. In retrospect, one recognizes from the present approach, that the additional Lagrangian multiplier h introduced in Guderley's paper will assume the value zero.

Method of Constructing Optimum Nozzle Contour

To illustrate the application of the solution given in the previous section toward obtaining a nozzle contour, a numerical example is carried out in detail in this section. A constant value of $\gamma = 1.23$ and zero ambient pressure are used in the example. The method is simple enough to make the appropriate changes for other conditions.

The first step is to choose a suitable curve for the nozzle wall contour in the throat region. A circular arc of radius $1.5y_t$ (y_t is the radius of throat section) is chosen for the nozzle contour upstream of the throat section. The asssumed nozzle wall contour in the throat region is shown in Fig. 2. Calculations according to (4) indicate a Mach number 1.103 on the wall at the throat section. In Fig. (2), TT' represents the line along which $M = 1.103$. The initial expansion im-

mediately behind the throat is assumed to occur along a circular arc of 0.45 y_t radius. Since flow across TT' is sufficiently supersonic, it is assumed unaffected by downstream conditions. A characteristic net is computed (see the section on initial expansion in the nozzle) for these initial conditions, a portion of which is shown in Fig. 2. The five right characteristic lines shown in the figure start from initial points on the nozzle wall in the throat region, where the wall slopes are 28, 30, 32, 34 and 35 deg, respectively.

Instead of choosing a particular nozzle length, M_E, the Mach number on the nozzle wall at the exit, will be prescribed. This Mach number forms a parameter which describes a posteriori the length of the nozzle. By choosing different values of M_E, optimum contours for different lengths can be obtained. Optimum nozzle contour for any particular desired length can then be obtained by interpolation. For zero ambient pressure, Equation [14] reduces to

$$\sin 2\theta_E = \frac{2}{\gamma M_E^2} \cot \alpha_E \quad \ldots\ldots\ldots\ldots [16]$$

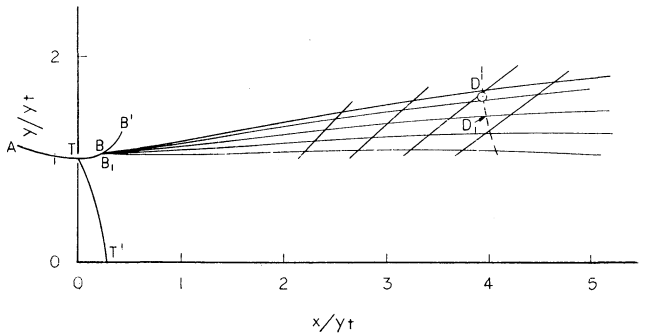

Fig. 2 Selection of the extent of initial expansion

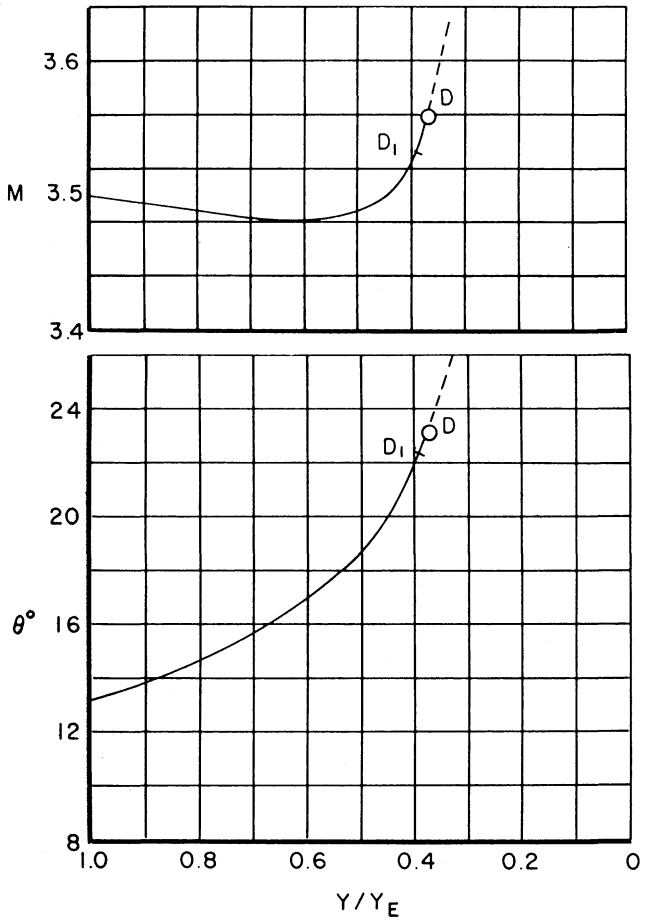

Fig. 3 Mach number and flow angle along the control surface

For the present numerical example $M_E = 3.5$ is chosen and the above equation yields the necessary wall slope $\theta_E = 13.22$ deg. Equations [12, 13] govern M and θ along the control surface, and the constants λ_2 and λ_3 can be evaluated by inserting $M_E = 3.5$ and $\theta_E = 13.22$ deg at $y = y_E$. Equations [12, 13] can be rewritten as

$$M^* \frac{\cos(\theta - \alpha)}{\cos \alpha} = M_E^* \frac{\cos(\theta_E - \alpha_E)}{\cos \alpha_E} \quad \ldots\ldots [17]$$

where

$$M^* = \left[\frac{1}{\gamma - 1 + \frac{2}{M^2}}\right]^{1/2}$$

and

$$\frac{y}{y_E} M^2 \left(1 + \frac{\gamma - 1}{2} M^2\right)^{-\gamma/(\gamma-1)} \sin^2 \theta \tan \alpha = M_E^2 \left(1 + \frac{\gamma - 1}{2} M_E^2\right)^{-\gamma/(\gamma-1)} \sin^2 \theta_E \tan \alpha_E \quad \ldots [18]$$

The above two equations can easily be solved by first choosing pairs of M, θ values satisfying Equation [17] and then obtaining corresponding values of y/y_E from Equation [18]. Fig. 3 shows the values of M and θ thus obtained as functions of y/y_E. These relations can be computed even though one does not yet know the position of the control surface DE (see Fig. 1).

The next step is to find the point in the characteristics net (shown in Fig. 2) which would define the end point on the control surface. Consider the flow conditions along the right characteristic from any point B_1 on the prescribed contour TB'. Pick a point D_1 on the right characteristic such that the values of M and θ at D_1 satisfy Equation [17]. The dashed line shown in the figure is the locus of all such points. From the values of M and θ at D_1, the value of y/y_E at D_1 can be found from Fig. 3. Conservation of mass requires the mass flow crossing the right characteristic B_1D_1 to be equal to the mass flow crossing the control surface from D_1 to E, the end point on the nozzle wall. That is

$$2\pi y_t^2 \rho_t W_t \int_{B_1}^{D_1} \frac{\rho W \sin \alpha}{\rho_t W_t \cos(\theta - \alpha)} \frac{y}{y_t} d\left(\frac{x}{y_t}\right) = 2\pi y_E^2 \rho_t W_t \int_1^{D_1} \frac{\rho W \sin \alpha}{\rho_t W_t \sin(\theta + \alpha)} \frac{y}{y_E} d\left(\frac{y}{y_E}\right) \quad \ldots [19]$$

It should be remembered that the integration on the left-hand side is carried out along B_1D_1 in Fig. 2, whereas the integration on the right-hand side depends upon the control surface, as described in Fig. 3, and the point D_1. Also the ratio of y_E/y_t in the above depends upon the choice of the point D_1.

The above equation can be satisfied by a few trials and by noting the error for each choice of the point D_1. In the present example the point D shown encircled in Figs. 2 and 3, satisfies the above equation, [19]. By interpolating between known right characteristics shown in Fig. 2, the right characteristic BD through the point D, with respective values of M and θ on it is found. This characteristic line BD is shown in Fig. 4, indicated as extent of "kernel" since the assumed initial expansion occurs up to this right line. The location of the point D as represented in Figs. 3 and 4 yields the ratio y_E/y_t. Equation [11] indicates that the control surface DE is a left characteristic and this property is used to find X/y_t for respective values of M, θ, and y/y_t along DE. Thus the information given in Fig. 3 can be translated to define the control surface DE in terms of y_t as shown in Fig. 4. The length of the nozzle is given by the x-coordinate of the point E and is found to be 8.19 y_t for this example.

Starting with the above derived flow conditions along lines

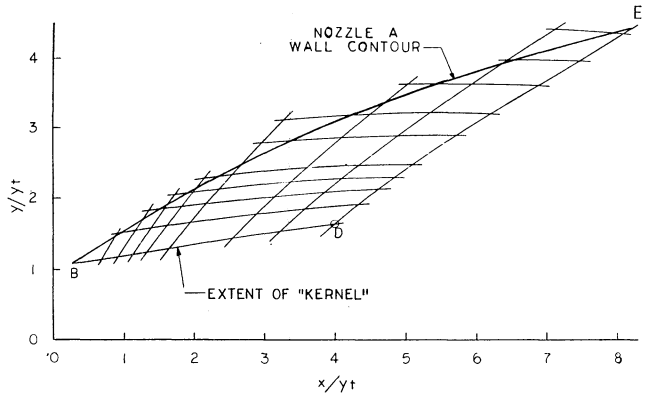

Fig. 4 Construction of the nozzle contour

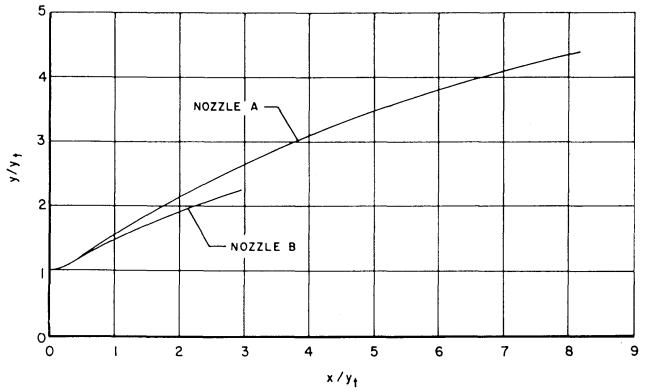

Fig. 5 Optimum nozzle contours—$P_a = 0$; $\gamma = 1.23$

BD and DE, the characteristics net is completed in the region between the two lines as shown in Figure 4. With the flow field in this region known, the streamline passing through B and E is drawn. This streamline shown in Fig. 4 then forms the required contour for nozzle length of 8.19 y_t. As mentioned before, optimum nozzle contours for different lengths can be designed by choosing different values for wall Mach number at the point E.

Typical Nozzle Configurations

The nozzle configuration computed in the preceding section is shown in Fig. 5 and represents the contour for optimum thrust when zero ambient pressure and a length of 8.19 y_t are prescribed. The coordinates of wall points, Mach number and wall slopes at the points are listed in Table 1. By choosing $M_E = 2.6$ and zero ambient pressure a shorter nozzle of length 2.94 y_t is designed and is also shown in Fig. 5. The coordinates of wall points of this nozzle are listed in Table 2.

Table 1 Optimum thrust nozzle A
($P_a = 0$, $\gamma = 1.23$, $L = 8.19 Y_t$)

X/Y_t	Y/Y_t	M	Wall slope θ, deg
0.25	1.08	2.11	34.4
0.33	1.13	2.19	32.8
0.94	1.52	2.42	32.0
1.03	1.58	2.45	31.7
1.17	1.66	2.48	31.2
1.47	1.84	2.57	30.4
1.88	2.07	2.67	29.0
2.31	2.30	2.77	27.5
3.37	2.82	2.96	24.0
4.20	3.16	3.08	21.6
5.43	3.32	3.24	18.5
6.50	3.95	3.35	16.2
7.98	4.34	3.48	13.5
8.19	4.40	3.50	13.1

Table 2 Optimum thrust nozzle B
($P_a = 0$, $\gamma = 1.23$, $L = 2.94 Y_t$)

X/Y_t	Y/Y_t	M	Wall slope θ, deg
0.21	1.05	1.96	28.7
0.29	1.10	2.01	27.8
0.63	1.27	2.12	26.9
0.91	1.41	2.20	26.1
1.52	1.70	2.34	23.7
2.30	2.01	2.49	20.4
2.94	2.23	2.60	17.9

The thrust coefficients of these nozzle configurations, computed from wall pressures, are shown in Table 3, and are compared with conical nozzles having the same lengths and area ratios. Thrust coefficient is defined as

$$C_T = \frac{\text{thrust}}{p_c A_t}$$

and the maximum attainable value depends only upon the ambient pressure and γ, the ratio of specific heats. For zero ambient pressure

$$C_{T_{\max}} = \gamma \left(\frac{\gamma+1}{2}\right)^{-\gamma/(\gamma-1)} \sqrt{\frac{\gamma+1}{\gamma-1}}$$

and one should remember that this value can only be obtained with a nozzle of infinite length and infinite exit area. The thrust coefficients of the optimum nozzles are also shown in Table 3 as percentages of the above maximum attainable value.

Table 3 Comparison of thrust coefficients

	Nozzle A of Fig. 5	Nozzle B of Fig. 5	Contour A shortened to length of nozzle B
Length-throat radius	8.19	2.94	2.294
Exit area-throat area	19.36	4.973	6.838
Thrust coefficient	1.7676	1.5829	1.5688
One-dimensional thrust for the area ratio, %	98.58	96.93	93.5
Thrust of conical nozzle of same length and area ratio, %	102.3	100.5	102.1
Maximum available thrust, %	82.7	74.1	73.4

Results presented in Table 3 show that nozzle A yields 2.3 per cent more thrust than a conical nozzle of the same length and area ratio. On the other hand, nozzle B, of much shorter length and smaller exit area, yields only 0.5 per cent more thrust than the equivalent conical nozzle. If nozzle contour A were cut off at a length of 2.94 y_t (i.e., the length of nozzle B) one obtains a thrust coefficient of 1.5688. As can be expected this value is lower than the thrust coefficient of the nozzle B which was designed to yield maximum thrust for the length.

To estimate the effect of γ on the optimum nozzle shape, $\gamma = 1.4$ is used, and for zero ambient pressure a nozzle is designed having a length of 9.19 y_t. This nozzle contour is shown in Fig. 6, and differs considerably from the contour computed for $\gamma = 1.23$. Increasing the value of γ reduces the exit area of optimum thrust nozzle.

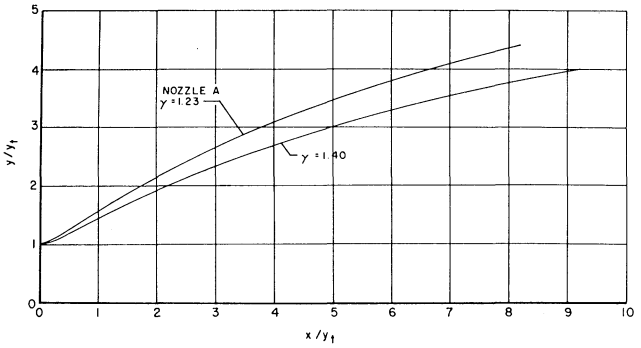

Fig. 6 Optimum nozzle contours—$P_a = 0$

It should be remembered that the nozzle contours shown in Figs. 5 and 6 are computed for inviscid isentropic flow. Similar to the methods used in wind tunnel nozzle design, one may compute the displacement thickness of the boundary layer along the nozzle wall and apply the correction to the contours shown in Figs. 5 and 6. Increasing the radial coordinates of the wall contour by the amount of the boundary layer thickness would yield the exit flow for which the nozzle is designed.

Conclusions

By applying the calculus of variations a method is developed for designing the wall contour of an optimum thrust nozzle. The ambient pressure, length of the nozzle and wall contour in the throat region appear as governing conditions in the formulation and solution of the problem. Typical nozzle contours are presented in Figs. 5 and 6.

A nozzle contour obtained for a given length and ambient pressure will also be the contour yielding maximum thrust when the length and the corresponding exit area are the prescribed conditions. For example, nozzle A shown in Fig. 5 will also be the optimum contour if, in addition to length of $L/y_t = 8.19$, an exit area of $A/A_t = 19.36$ is the condition prescribed in place of zero ambient pressure.

The nozzle contours presented in Fig. 5 show the difference between the optimum nozzles computed for the two different lengths. On the contrary, Guderley and Hantsch (4) concluded from their computations that for a given ambient pressure all optimum nozzles of different lengths can be represented by a single contour. This may be a coincidence due to either the sharp-corner expansion he considered, or the complicated nature of his solution.

The ratio of specific heats, γ, of the exhaust gases has considerable effect on the optimum nozzle contour as can be seen from Fig. 6.

Comparison of thrust coefficients shown in Table 3 indicates that the advantage of contoured nozzles is greater at larger area ratios.

References

1 Foelsch, K., "The Analytical Design of an Axially Symmetric Laval Nozzle for a Parallel and Uniform Jet," *Journal of the Aeronautical Sciences*, March 1949.

2 Dillaway, R. B., "A Philosophy for Improved Rocket Nozzle Design," JET PROPULSION, vol. 27, Oct. 1957, p. 1088.

3 Fraser, R. P., and Rowe, P. N., "The Design of Supersonic Nozzles for Rockets," Imperial College of Science, South Kensington, England, Report JRL No. 28, Oct. 1954.

4 Guderley, G., and Hantsch, E., "Beste Formen für Achsensymmetrische Uberschallschubdusen," *Zeitschrift für Flugwissenschaften*, Brauschweig, Sept. 1955.

5 Sauer, R., "General Characteristics of Flow Through Nozzles at Near Critical Speeds," NACA TM 1147.

6 Shapiro, A. H., "The Dynamics and Thermodynamics of Compressible Fluid Flow," Ronald Press, New York, pp. 676–680.

Prediction of the Explosive Behavior of Mixtures Containing Hydrogen Peroxide

E. S. SHANLEY[1] and J. R. PERRIN[2]

Becco Chemical Division, Food Machinery & Chemical Corporation, Buffalo, N. Y.

This paper concerns a relationship between thermal properties and explosive properties for mixtures containing hydrogen peroxide, water and soluble organic compounds. It has been known for some time that certain mixtures of this kind are explosive. In the present study it has been found that sensitivity to initiation is about the same for all mixtures having the same heat of reaction. This relationship is demonstrated for five different organic constituents and for three methods of initiation. The findings provide an easy basis for predicting the likely range of explosive compositions of untested mixtures containing hydrogen peroxide.

Introduction

TERNARY mixtures containing hydrogen peroxide, water and soluble organic compounds are used in rocket propulsion, in synthetic organic chemistry, and for other purposes. Mixtures of this kind are explosive within certain concentration limits. The range of explosive compositions has been determined empirically in a few cases.[3] This is a laborious undertaking, so that a way was sought to predict the properties of untested mixtures. The present communication shows the correlation found between explosive behavior and ΔH, the calorimetric heat of reaction. This correlation can be used to predict the range of explosive compositions for untested mixtures.

Experimental Part

Mixtures containing hydrogen peroxide, water and several different combustible materials were tested. Only soluble "fuels" were used, so as to avoid the complications of two-phase systems. Tests for sensitivity were carried out with blasting caps, drop weights and static sparks, as described

Received Sept. 9, 1957.

[1] Present address: Arthur D. Little, Inc., Cambridge, Mass. Mem. ARS.

[2] Present address: Marquardt Aircraft Company, Van Nuys, Calif.

[3] Shanley, E. S., and Greenspan, F. P., "Highly Concentrated Hydrogen Peroxide," *Ind. Eng. Chem.*, vol. 39, 1947, pp. 1536–1543.